

# Structural stability of poly(3-methylthiophene) and poly(3,4-ethylenedioxythiophene) in the ITO/PEDOT:PSS/P3MT system

Aline Domingues Batista<sup>1</sup> · Danielly Cristina Bento<sup>1</sup> · Henrique de Santana<sup>1</sup> 

Received: 29 July 2016 / Accepted: 3 September 2016 / Published online: 7 September 2016  
© Springer Science+Business Media New York 2016

**Abstract** With the aim of understanding the factors that enhance the efficiency of Organic photovoltaic cells (OPVs), poly(3-methylthiophene) (P3MT) was anodically deposited (+1.65 V vs Ag/AgCl) on ITO coated with poly(3,4-ethylenedioxythiophene) doped with poly(4-styrenesulfonate) (ITO/PEDOT:PSS) in LiClO<sub>4</sub>-ACN. This active layer was studied by ex situ Raman spectroscopy as a function of time, and led us to the conclusion that the radical cation species in the P3MT thiophene ring was very stable compared the ITO/P3MT system. Bearing in mind that P3MT synthesis on ITO/PEDOT:PSS occurs at high anodic potential, the behavior of the PEDOT at the applied potential was verified by electrochemical impedance spectroscopy and in situ Raman spectroscopy of the PEDOT:PSS on Pt. The Bode phase plots at potentials of −0.60, 0.00, 0.40, 0.60 and 0.80 V for the Pt/PEDOT:PSS/LiClO<sub>4</sub>-ACN system showed the contributions of the polaron and bipolaron conduction of the PEDOT thiophene ring. To back up this study, in situ Raman spectroscopy was used at the same potentials to verify the characteristic frequencies of the radical cation and dication species of the PEDOT thiophene ring. These results provided a basis for determining that the radical cation form of the PEDOT thiophene ring was the same stable form at the PEDOT:PSS/P3MT interface, which could enhance charge injection processes in OPVs.

## 1 Introduction

Poly(3-alkylthiophenes) (P3ATs) are important conjugated polymers, used in organic optoelectronics, mainly in Organic photovoltaic cells (OPVs) [1–5] because of their relatively high charge mobility [6]. However, these devices have not lived up to expectations due to the loss of absorbed photons caused by the formation of the donor exciton at a distance greater than its diffusion length [7, 8]. To overcome this problem, some chemical modifications to these polymers have been investigated, such as the synthesis of copolymers using P3ATs with other conjugated polymers [1, 6, 8–12].

The use of poly(3,4-ethylenedioxythiophene) doped with poly(4-styrenesulfonate) (PEDOT:PSS) and P3ATs forming a hole injection layer in OPVs has improved device efficiency because it accepts holes from any polymer, irrespective of the highest occupied molecular orbital (HOMO). In a OPV device in which P3HT has a work function very close to that of PEDOT:PSS, the contact seems to be ohmic and occurs without net energy loss [13–15].

Huang et al. [13] used P3HT/PCBM deposited on PEDOT:PSS as bulk-heterojunction layers. After heat-treating this material, the formation of a P3HT<sup>+</sup> doped with PSS<sup>−</sup> was proposed, in order to affect the open-circuit voltage and increase the compensation voltage in this mixed layer.

In our study, a film of poly(3-methylthiophene) (P3MT) electrochemically prepared on ITO/PEDOT:PSS, with emphasis on the structural characterization of the P3MT and PEDOT in the ITO/PEDOT:PSS/P3MT system. This system was monitored as a function of time by ex situ Raman spectroscopy and compared to the behavior of P3MT deposited on ITO. To study the behavior of the

✉ Henrique de Santana  
hensan@uel.br

<sup>1</sup> Departamento de Química - CCE, Universidade Estadual de Londrina, Londrina, PR 86051-990, Brazil

PEDOT at the interface with the P3MT, in situ Raman spectroscopy and electrochemical impedance spectroscopy (EIS) were necessary to verify the behavior of the PEDOT as a function of the applied potential, bearing in mind that P3MT film synthesis occurred at more anodic potentials on the ITO/PEDOT:PSS system.

Examining the EIS data using a Bode phase plot helped identify the charge transfer processes in which low frequency processes can be associated with polaron conduction (radical cation) and bipolaron conduction (dication), helping to characterize the structure of the PEDOT when the P3MT synthesis potential was applied. In conjunction with EIS, in situ Raman spectroscopy with application of the potential was used with the aim of characterizing and confirming the stabilization of radical cation and dication species in the PEDOT polymer matrix in comparison to its structure in the ITO/PEDOT:PSS/P3MT system.

## 2 Experimental

### 2.1 Reagents

The monomer, 3-methylthiophene ( $C_5H_7S$ ) and the Poly(3,4-ethylenedioxythiophene)-poly(styrenesulfonate) (PEDOT:PSS) were obtained from Aldrich and used as received. The support electrolyte was 99 % lithium perchlorate ( $LiClO_4$ ), supplied by Acros Organics. The 99.5 % HPLC acetonitrile ( $CH_3CN$ ) was obtained from JT Baker.

### 2.2 Electrochemical synthesis

The PEDOT:PSS, 0.8 % in  $H_2O$ , was first dispersed on Pt or ITO (sheet resistance 8–12  $\Omega^2$ ) by painter method. It was dried at 70 °C for 5 min to produce the Pt/PEDOT:PSS or ITO/PEDOT:PSS system. The P3MT was synthesized electrochemically on ITO/PEDOT:PSS by applying a potential of +1.65 V for 70 s in a 0.035 mol  $L^{-1}$  solution of 3-methylthiophene in  $LiClO_4$ -ACN, producing the ITO/PEDOT:PSS/P3MT system over an average area of 0.30  $cm^2$ . This was done by means of chronoamperometry (CA) using an Autolab PGSTAT 302 N potentiostat/galvanostat coupled to a microcomputer running NOVA 1.8 A 0.50  $cm^2$  platinum plate was used as the auxiliary electrode. Potentials were determined by reference to Ag/AgCl in a Luggin capillary in a 0.100 mol  $L^{-1}$  solution of  $LiClO_4$  in acetonitrile ( $LiClO_4$ -ACN).

### 2.3 Raman spectroscopy

Ex situ Raman spectra were obtained on a DeltaNu Advantage532<sup>®</sup> portable Raman spectrometer, excited at 532 nm with resolution of 8  $cm^{-1}$ . DeltaNu NuSpec

software was used with baseline resources to remove background fluorescence. A WITec alpha 300 s spectrometer was also used ( $\lambda_{exc} = 785$  nm, 10  $\mu m$  diameter spot, typical exposure time 10 min).

To obtain in situ Raman spectra, potentials of  $-0.60$ ,  $0.00$ ,  $+0.40$ ,  $+0.60$  and  $+0.80$  V were applied by means of a Microquímica MQPG-01 potentiostat coupled to a microcomputer. The potentials were applied by reference to Ag/AgCl in a Luggin capillary in a 0.100 mol  $L^{-1}$  solution of  $LiClO_4$ -ACN.

### 2.4 Electrochemical impedance spectroscopy (EIS)

To obtain impedance diagrams at different potentials, an Autolab PGSTAT 302 NP was used with the FRAM32 impedance module, varying the frequency from 100 kHz to 0.01 Hz. The following potentials were applied:  $-0.60$ ,  $0.00$ ,  $+0.40$ ,  $+0.60$  and  $+0.80$  V. The diagrams were recorded after waiting time of 15 min, necessary to attain the stationary state at which the current is constant.

## 3 Results and discussion

Figure 1 shows the ex situ Raman spectra as a function of time for the P3MT film, beginning soon after electrical synthesis under the ITO electrode and in a solution of  $LiClO_4$ -ACN.

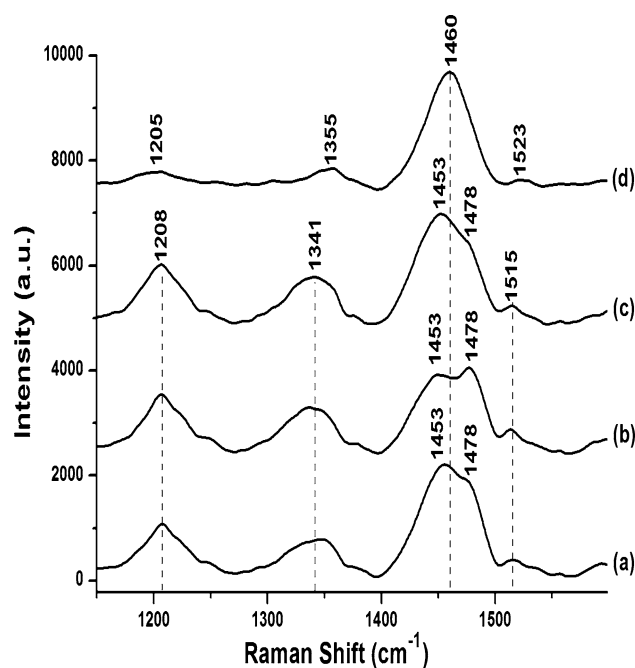


**Fig. 1** Ex situ Raman spectra as a function of time for the ITO/P3MT system previously prepared by electrochemical means in a  $LiClO_4$ /ACN medium, at 532 nm excitation radiation and at the following times: *a* as prepared, *b* after 1 h, *c* after 2 h and *d* after 18 h

The bands observed at 1205–1208, 1341–1355, 1460 and 1515–1523  $\text{cm}^{-1}$  were attributed to  $\text{C}-\text{C}_{\text{inter-ring}}$  stretching,  $\text{C}-\text{C}_{\text{ring}}$  stretching,  $\text{C}=\text{C}_{\text{ring}}$  symmetric stretching and  $\text{C}=\text{C}_{\text{ring}}$  asymmetric stretching, in line with Louarn et al. [16]. A wider band centered on 1460  $\text{cm}^{-1}$  was observed in all spectra. In the spectra as prepared and at 1 and 2 h after P3MT synthesis, the formation of shoulders at 1453 and 1478  $\text{cm}^{-1}$  were observed, but these shoulders were not observed after 18 h. These changes over time could be indicative of a change in the thiophene ring from aromatic to quinoidal (radical cation or dication) [5, 17–20].

To better understand this behavior, it was necessary to deconvolute the Raman spectra between 1400 and

1500  $\text{cm}^{-1}$ , a region sensitive to changes in the thiophene ring [21].

Figure 2a–c show the deconvoluted Raman spectra for the ITO/P3MT system, obtained from the films as prepared and at 1 and 2 h after synthesis. The bands at 1426–1430, 1450–1460 and 1477–1480  $\text{cm}^{-1}$  were of different relative intensities, phenomena attributed respectively to the aromatic, dication and radical cation species [22]. In the deconvoluted spectrum obtained as prepared and at 1 h after P3MT synthesis, the relative intensities of the bands at 1450–1454 and 1477–1480  $\text{cm}^{-1}$  were close. At 2 h after P3MT synthesis, deconvolution of the Raman spectrum showed bands at 1426, 1454 and 1480  $\text{cm}^{-1}$ . The

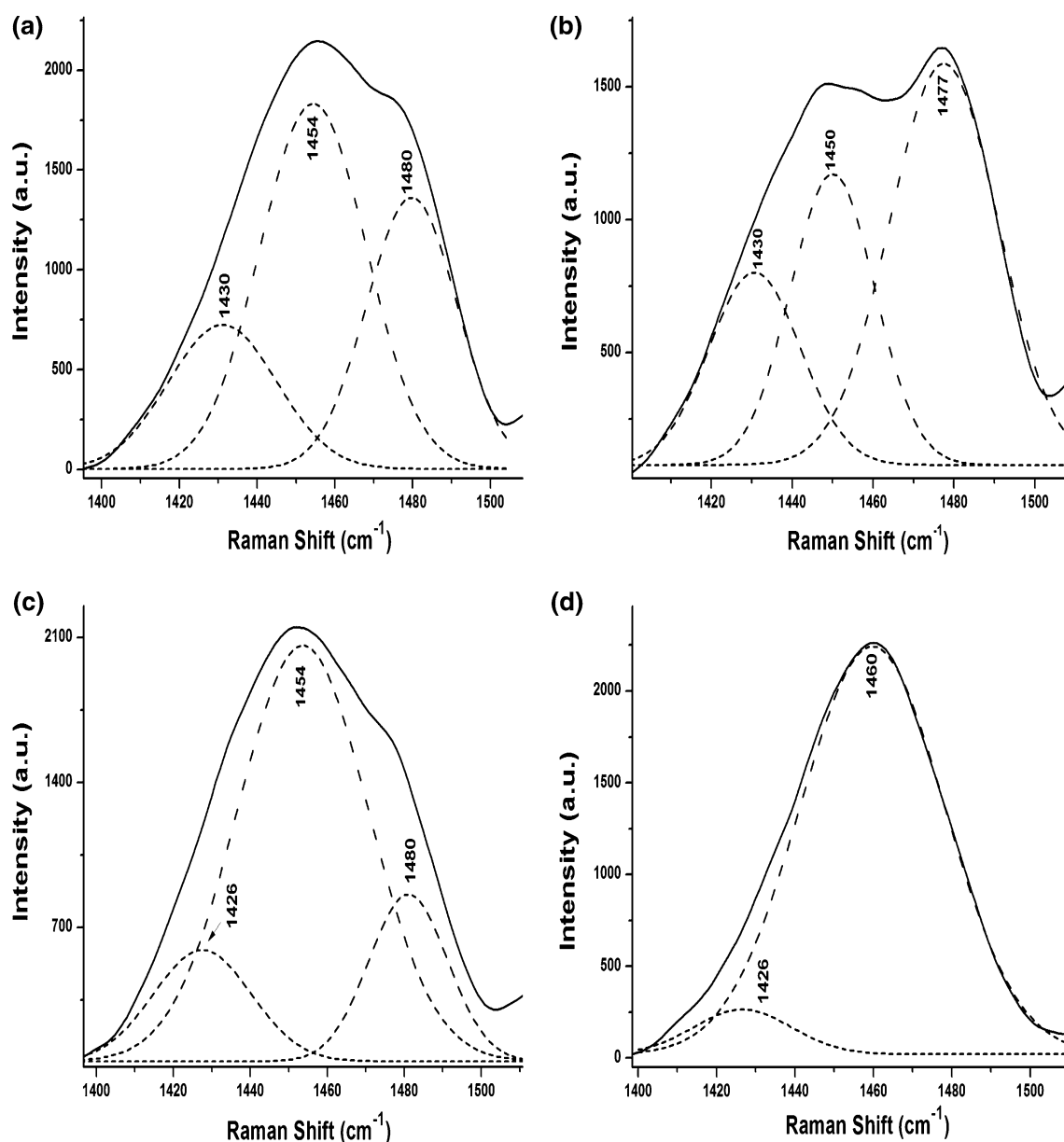


**Fig. 2** Ex situ deconvoluted Raman spectra as a function of time in the 1400–1500  $\text{cm}^{-1}$  region of P3MT films synthesized on ITO **a** as prepared, **b** after 1 h, **c** after 2 h and **d** after 18 h

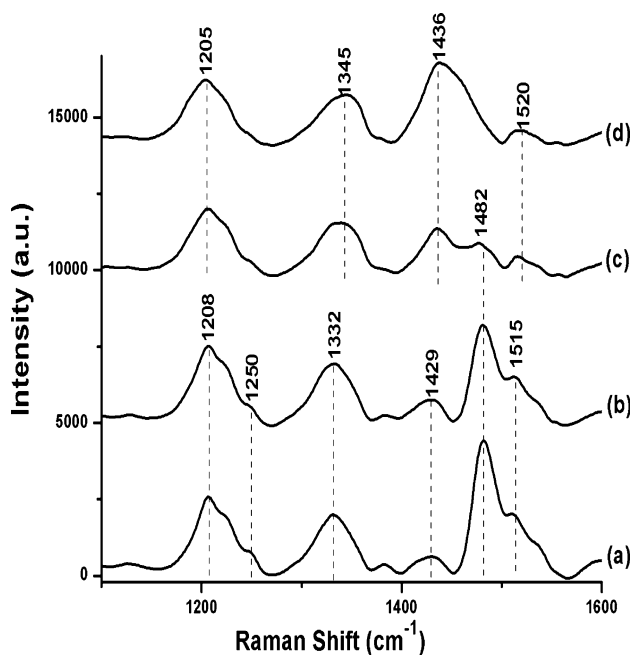
most intense of these three bands was the one at  $1454\text{ cm}^{-1}$ , related to the dication species.

Figure 2d shows that the deconvoluted spectrum obtained at 18 h after synthesis of the P3MT film no longer contains the band related to the radical cation, and instead contains bands at  $1426$  and  $1460\text{ cm}^{-1}$  attributed to the aromatic and dication segments. The band related to the dication is the most intense.

These results show that the radical cation species in the P3MT film matrix on ITO is stable for only 2 h. This occurred because of the spontaneous disproportioning of the radical cation in aromatic and dication segments, corroborating the literature on polydiphenylamine [23]. Working on P3ATs, Koizumi et al. [24] stated that these polymers could undergo natural dedoping as time progresses, caused by the instability of the material due to its polymer nature, the length of the alkyl chain, humidity and the atmospheric conditions to which the film was subjected.

Figure 3 shows Raman spectra of the ITO/PEDOT:PSS/P3MT system as a function of time. The PEDOT:PSS was initially deposited on the ITO electrode and then the P3MT film electrochemically synthesized by applying a potential of  $+1.65\text{ V}$  to the PEDOT:PSS system in a  $\text{LiClO}_4/\text{ACN}$  medium.

Main bands at  $1208$ ,  $1332$ ,  $1429$ ,  $1482$  and  $1515\text{ cm}^{-1}$  were observed in the spectrum for the ITO/PEDOT:PSS/P3MT as prepared. As time progressed, these bands shifted and became wider. After 19 h, there was a drastic reduction



**Fig. 3** Ex situ Raman spectra as a function of time for the ITO/PEDOT:PSS/P3MT system at  $532\text{ nm}$  excitation radiation and at the following times: *a* as prepared, *b* after 1 h, *c* after 19 h and *d* after 25 h

in the intensity of the band at  $1482\text{ cm}^{-1}$  and after 25 h in the predominance of the bands at  $1205$ ,  $1345$ ,  $1436$  and  $1520\text{ cm}^{-1}$ , and in particular, the formation of a wide band centered on  $1436\text{ cm}^{-1}$ .

Figure 4 shows the deconvoluted Raman spectra as a function of time for the ITO/PEDOT:PSS/P3MT system.

Figure 4a, b, shows the deconvoluted Raman spectra for the system as prepared and after 1 h, with the frequencies at  $1429$ ,  $1479$  and  $1510\text{ cm}^{-1}$ . They include a wide band at  $1429\text{ cm}^{-1}$  attributed to symmetric C=C stretching of the PEDOT thiophene ring [25], and wide bands at  $1479$  and  $1510\text{ cm}^{-1}$  attributable respectively to symmetric and asymmetric C=C stretching related to the P3MT thiophene ring [5, 16–20]. The band at  $1479\text{ cm}^{-1}$  was more intense at both evaluation times.

Figure 4c, d, showing the deconvoluted Raman spectra for the system after 19 and 25 h, reveal a drop in the relative intensity of the band at  $1479\text{ cm}^{-1}$  compared to the band at  $1436\text{ cm}^{-1}$ . There is also an increase in intensity and shifting of the band at  $1510$ – $1517\text{ cm}^{-1}$  that could be attributed to asymmetric C=C stretching of the PEDOT thiophene ring [25].

This behavior of the ITO/PEDOT:PSS/P3MT system as time progresses has never been observed in the Raman spectrum of the ITO/P3MT system (Fig. 2), which shows that, after 4 h, the bands of the radical cation segments were of low intensity and the band of the aromatic and dication species were predominant after longer times had elapsed.

As detailed in the experimental part of this study, the P3MT film on the PEDOT:PSS system, previously deposited on ITO, was produced electrochemically by applying a potential of  $+1.65\text{ V}$ . This procedure for depositing P3MT on the ITO/PEDOT:PSS system probably also oxidizes the PEDOT thiophene ring. If this is the case, attributing the band at  $1435\text{ cm}^{-1}$  to symmetric C=C stretching of the PEDOT thiophene ring could be better described as a function of the quinoidal segments and not just in terms of the thiophene ring aromatic structure.

In line with the work of Garreau et al. [25], the in situ Raman spectrum of the PEDOT showed a frequency at  $1423\text{ cm}^{-1}$  attributed to C=C stretching of the PEDOT thiophene ring. This band shifted to  $1411\text{ cm}^{-1}$  with the application of a  $-0.30\text{ V}$  potential, to  $1431\text{ cm}^{-1}$  with the application of  $+0.30\text{ V}$  and to  $1450\text{ cm}^{-1}$  with the application of  $+0.80\text{ V}$ .

Experiments were therefore carried out on the Pt/PEDOT:PSS system in order to verify the behavior of quinoidal species in the PEDOT thiophene ring at the potential applied.

Figure 5 shows the Bode phase plots at potentials of  $-0.60$ ,  $0.00$ ,  $0.40$ ,  $0.60$  and  $0.80\text{ V}$  applied to the Pt/PEDOT:PSS/ $\text{LiClO}_4$ -ACN system, comparing the

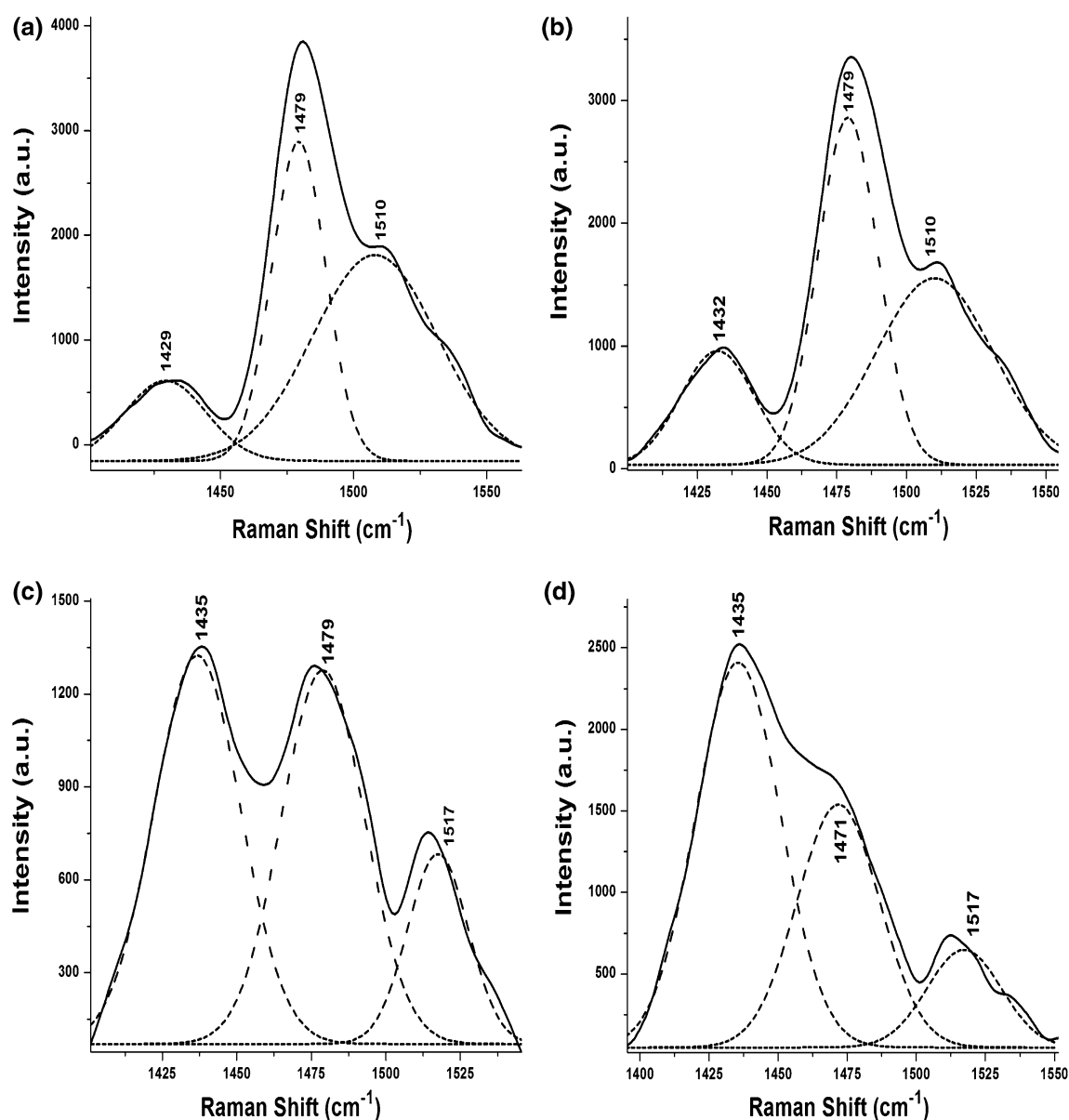


**Fig. 4** Ex situ deconvoluted Raman spectra as a function of time for the ITO/PEDOT PSS/P3MT system and at the following times: **a** as prepared, **b** after 1 h, **c** after 18 h and **d** after 26 h

closeness of these plots to the results of Garreau et al. [25] by cyclic voltammetry, in which there are oxidation peaks not clearly defined and centered approximately at  $-0.10$  and  $+0.55$  V on the platinum electrode (E vs Ag/AgNO<sub>3</sub>/(TBA)BF<sub>4</sub>-ACN). According to the authors, the PEDOT can behave in a similar way to polythiophene, in which the first anodic peak occurs on the formation of the radical cation and the second peak on stabilization of the dication form of the thiophene ring.

IES was used to obtain the Bode phase plots, since this technique permits the phases present at the different time constants to be determined for the conductor electrode/doped polymer system. At low frequencies, the

process is generally observed to take place in two stages, relating to swings in the radical cation (polaron) and dication (bipolaron) species in the polymer matrix, and to electronic conduction at high frequencies [26]. This behavior was also observed at the interface of P3ATs deposited on the polydiphenylamine coating the platinum electrode [22, 27–29].

The Bode phase plots of the Pt/PEDOT:PSS/LiClO<sub>4</sub>-ACN system (Fig. 5) when potentials of  $-0.60$  or  $0.00$  V were applied show the respective phases at the different time constants centered on 0.04 or 0.06 Hz, relating to polaron conduction. When a potential of 0.40 V is applied, the phase shifts to the time constant at 0.23 Hz and when

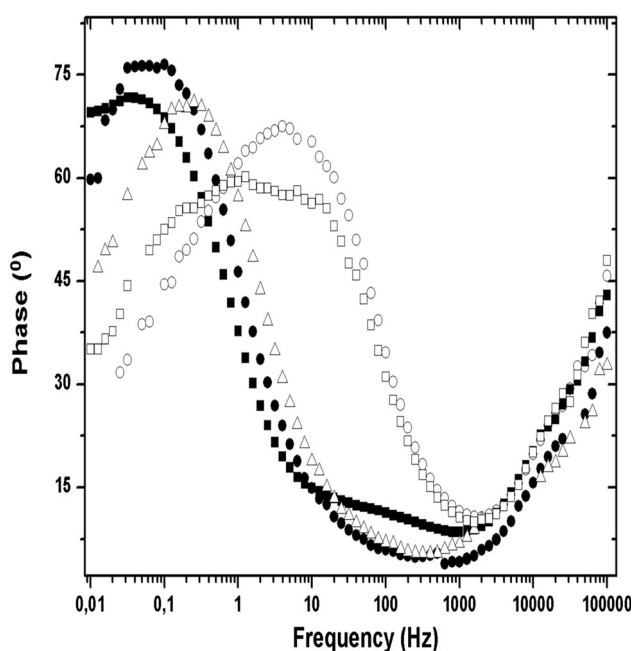


**Fig. 5** Bode phase plots for the Pt/PEDOT:PSS/LiClO<sub>4</sub>-ACN system produced by applying the following potentials: (filled square)  $-0.60$  V; (filled circle)  $0.00$  V; (open triangle)  $+0.40$  V; (open square)  $+0.60$  V; (open circle)  $+0.80$  V

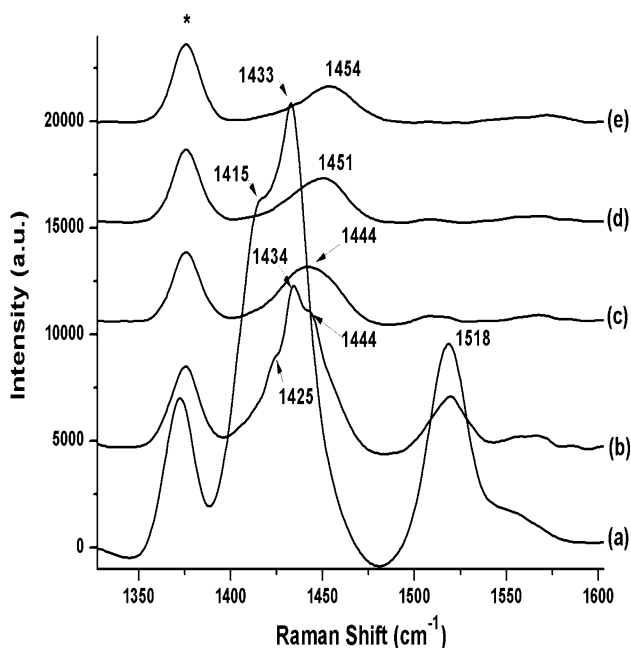


**Fig. 6** In situ Raman spectrum of the PEDOT:PSS deposited on platinum at  $532$  nm excitation radiation and at the following potentials: *a*  $-0.60$  V, *b*  $0.00$  V, *c*  $+0.40$  V, *d*  $+0.60$  V and *e*  $+0.80$  V. (Asterisk) characteristic acetonitrile band

$0.60$  V is applied, a wide phase forms, centered around  $4.50$  Hz and relating to simultaneous polaron and bipolaron conduction. At  $0.80$  V, the phase at  $4.50$  Hz narrows, perhaps due to improved bipolaron conduction.

Figure 6 shows the in situ Raman spectra for the Pt/PEDOT:PSS/LiClO<sub>4</sub>-ACN system, in order to characterize the frequencies of the radical cation and dication species at the applied potential, based on the results in the Bode phase plots.

Figure 6 shows in situ Raman spectra at potentials of  $-0.60$ ,  $0.00$ ,  $+0.40$ ,  $+0.60$  and  $+0.80$  V, revealing spectral variations mainly in the region of  $1390$ – $1560$  cm<sup>-1</sup>, attributed to C=C stretching of the PEDOT thiophene ring. These results indicate that the PEDOT polymer matrix may be undergoing structural changes in the thiophene ring as a function of the applied potential, which could define the structure of the PEDOT when subjected to the potential for synthesizing the P3MT on ITO/PEDOT:PSS, as discussed above in regard to Fig. 4.

The in situ Raman spectrum of the PEDOT:PSS obtained at a potential of  $-0.60$  V (Fig. 6a) in a LiClO<sub>4</sub>-ACN medium shows a band at  $1376$  cm<sup>-1</sup> attributed to the solvent, and intense bands at  $1433$  and  $1518$  cm<sup>-1</sup> attributed respectively to symmetric and asymmetric C=C stretching of the PEDOT thiophene ring [25]. A shoulder is also present at  $1415$  cm<sup>-1</sup>.

In the spectral region attributed to symmetric C=C stretching of the PEDOT thiophene ring on applying a potential of  $0.00$  V (Fig. 6b), the band at  $1434$  cm<sup>-1</sup> remains intense and a shoulder was observed at  $1444$  cm<sup>-1</sup>, together with a drop in the intensity of the band at  $1518$  cm<sup>-1</sup>. As the potential is increased from  $+0.40$  to  $+0.80$  V (Fig. 6c–e), a low intensity band at  $1454$  cm<sup>-1</sup> stabilizes. The shifts observed in the in situ Raman spectra as the potential is varied are similar to those reported by Garreau et al. [25].

Compared to the electrochemical spectrum results at the same potentials observed in the Bode phase plots, the intense band at  $1433$  cm<sup>-1</sup> at potentials between  $-0.60$  and  $0.00$  V could be related to the stabilization of the radical cation species. In contrast, the dication species in the PEDOT matrix reaches stabilization at  $0.60$  V and this species could be related to the band observed at  $1454$  cm<sup>-1</sup>.

These results complement the work of Garreau et al. [25] and Sakamoto et al. [30]. Both authors found that the absorption band in the neutral form of PEDOT ( $E < -0.20$  V) was present in the visible region, with the maximum at close to  $600$  nm, corresponding to the  $\pi$ - $\pi^*$  transition. In view of this, the species that showed the intense band at  $1433$  cm<sup>-1</sup>, observed in our system between  $-0.60$  and  $0.00$  V, can be considered responsible for absorption at  $600$  nm. Therefore, the most intense band would be shown in the resonant Raman effect when excited at radiation of  $532$  nm. In contrast, the shoulder observed at  $1415$  cm<sup>-1</sup> must be associated with the neutral form of the thiophene ring in the PEDOT present in the polymer

structure, due to the fact that the PEDOT dedoping process apparently does not occur easily, even at more cathodic potentials.

During the oxidation process, Garreau et al. [25] and Sakamoto et al. [30] observed that the band around 600 nm decreases and the polymer starts to absorb in the infrared region, between 800 and 1200 nm. In terms of our results, when potentials higher than 0.00 V are applied, the dication-related band at  $1454\text{ cm}^{-1}$  was of low intensity because it did not undergo the resonant Raman effect. To observe the resonant Raman effect in this species, we obtained resonance Raman spectra by excitation at 785 nm.

Figure 7 shows ex situ Raman spectra at 785 nm excitation for the PEDOT:PSS system deposited on the platinum electrode as prepared and the same system after application of +1.65 V. After applying this potential, the electrode was removed from the electrolyte solution to record the spectrum.

The Raman spectrum in Fig. 7a for the PEDOT:PSS deposited on platinum shows the band at  $1433\text{ cm}^{-1}$ , related to the radical cation in the PEDOT thiophene ring, due to PSS doping. In contrast, the Raman spectrum for the Pt/PEDOT:PSS system in Fig. 7b, even at a potential of +1.65 V, still shows an intense band at  $1454\text{ cm}^{-1}$  characterizing dication stabilization in the PEDOT thiophene ring as a result of the potential applied. This could indicate that when the P3MT is electrochemically synthesized on the Pt/PEDOT:PSS system, the PEDOT is not degraded by the excessive overvoltage.

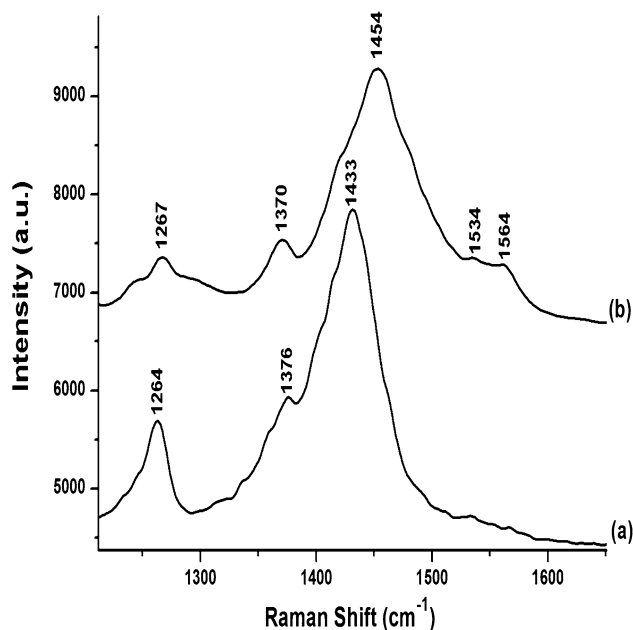


**Fig. 7** Ex situ Raman spectrum of the PEDOT:PSS deposited on platinum *a* as prepared and *b* after applying a potential of +1.65 V. Excitation radiation: 785 nm

## 4 Conclusion

P3MT behavior as a function of time, observed in the ITO/PEDOT:PSS/P3MT system as the presence of a persistent band at  $1479\text{ cm}^{-1}$  in the ex situ Raman spectrum, shows that there is greater stabilization of the P3MT radical cation species under ambient conditions compared to its stabilization in the ITO/P3MT system.

It was also verified that the PEDOT film was highly electroactive when the potential was applied to the platinum electrode, forming the radical cation and dication species in distinct potentials. This behavior makes it easier to define the characteristic bands of these two segments formed in the PEDOT matrix using in situ Raman spectroscopy, complemented by IES data.

These findings could also be applied to the characterization of the ITO/PEDOT:PSS/P3MT system matrix, in which the radical cation species in the thiophene rings of both PEDOT and P3MT are segments stabilized at this interface, which should facilitate the extraction of holes and increase the efficiency of organic solar cells.

**Acknowledgments** We would like to express our appreciation to the Spectroscopy Laboratory (SPEC) at the PROPPG/UEL Multiuser Center and the National Council for Scientific and Technological Development (CNPq) for their financial support (Project No. 441689/2014-0). D.C. Bento is indebted to the Coordination for the Improvement of Higher Education Personnel (CAPES) for the grant.

## References

1. E. Zhou, Z. Tan, Y. He, C. Yang, Y. Li, J. Polym. Sci., Part A: Polym. Chem. **45**, 629 (2007)
2. W.D. Feng, Z.J. Qi, Y.M. Sun, Eur. Polym. J. **43**, 3638 (2007)
3. T.N.M. Cervantes, D.C. Bento, E.C.R. Maia, D.A.M. Zaia, E. Laureto, M.A.T. Silva, G.J. Moore, H. de Santana, J. Mater. Sci.: Mater. Electron. **23**, 1916 (2012)
4. M.-C. Chen, S. Kar, D.-J. Liaw, W.-H. Chen, Y.-C. Huang, Y. Tai, Org. Electron. **13**, 2702 (2012)
5. D.C. Bento, E.C.R. Maia, P.R.P. Rodrigues, G. Louarn, H. de Santana, J. Mater. Sci.: Mater. Electron. **24**, 4732 (2013)
6. Y. Li, L. Xue, H. Xia, B. Xu, S. Wen, W. Tian, J. Polym. Sci., Part A: Polym. Chem. **46**, 3970 (2008)
7. Y.-J. Cheng, S.-H. Yang, C.-S. Hsu, Chem. Rev. **109**, 5868 (2009)
8. W. Lee, H. Choi, S. Hwang, J.Y. Kim, H.Y. Woo, Chem. Eur. J. **18**, 2551 (2012)
9. L.-M. Chen, Z. Hong, G. Li, Y. Yang, Adv. Mater. **21**, 1434 (2009)
10. Y. He, W. Wu, Y. Liu, Y. Li, J. Polym. Sci., Part A: Polym. Chem. **47**, 5304 (2009)
11. Q. Zhang, A. Cirpan, T.P. Russell, T. Emrick, Macromolecules **42**, 1079 (2009). (Washington, DC, U. S.)
12. K. Lu, X. Sun, Y. Liu, C. Di, H. Xi, G. Yu, X. Gao, C. Du, J. Polym. Sci., Part A: Polym. Chem. **7**, 1381 (2009)
13. D.M. Huang, S.A. Mauger, S. Friedrich, S.J. George, D. Dumitriu-LaGrange, S. Yoon, A.J. Moulé, Adv. Funct. Mater. **21**, 1657 (2011)

14. F. Zhang, A. Vollmer, J. Zhang, Z. Xu, J.P. Rabe, N. Koch, *Org. Electron.* **8**, 606 (2007)
15. G. Heimel, I. Salzmann, S. Duhm, J.P. Rabe, N. Koch, *Adv. Funct. Mater.* **19**, 3874 (2009)
16. G. Louarn, J. Mevellec-Y, J.P. Buisson, S. Lefrant, *Synth. Met.* **55**, 587 (1993)
17. S. Lefrant, I. Baltog, M.L. de la Chapelle, M. Baibarac, G. Louarn, C. Journet, P. Bernier, *Synth. Met.* **100**, 13 (1999)
18. T.N.M. Cervantes, D.C. Bento, E.C.R. Maia, R.V. Fernandes, E. Laureto, G.J. Moore, G. Louarn, H. De Santana, *J. Mater. Sci.: Mater. Electron.* **25**, 1703 (2014)
19. D.C. Bento, E.A. Da Silva, C.A. Olivati, G. Louarn, H. De Santana, *J. Mater. Sci.: Mater. Electron.* **26**, 7844 (2015)
20. H. De Santana, E.C.R. Maia, D.C. Bento, T.N.M. Cervantes, G.J. Moore, *J. Mater. Sci.: Mater. Electron.* **24**, 3352 (2013)
21. E.C.R. Maia, D.C. Bento, E. Laureto, D.A.M. Zaia, E.M. Therezio, G.J. Moore, H. de Santana, *J. Serb. Chem. Soc.* **78**, 507 (2013)
22. D.C. Bento, E.C.R. Maia, T.N.M. Cervantes, C.A. Olivati, G. Louarn, H. De Santana, *J. Mater. Sci.: Mater. Electron.* **26**, 149 (2015)
23. H. de Santana, M.L.A. Temperini, J.C. Rubim, *J. Electroanal. Chem.* **356**, 145 (1993)
24. H. Koizumi, H. Dougauchi, T. Ichikawa, *J. Phys. Chem. B.* **109**, 15288 (2005)
25. S. Garreau, G. Louarn, J.P. Buisson, G. Froyer, S. Lefrant, *Macromolecules* **32**, 6807 (1999). (**Washington, DC, U. S.**)
26. G. Lillie, P. Payne, P. Vadgama, *Sens. Actuators, B* **78**, 249 (2001)
27. K. Marumoto, N. Takeuchi, T. Ozak, S. Kuroda, *Synth. Met.* **129**, 239 (2002)
28. D.C. Bento, E.C.R. Maia, R.V. Fernandes, E. Laureto, G. Louarn, H. de Santana, *J. Mater. Sci.: Mater. Electron.* **25**, 185 (2014)
29. D.C. Bento, G. Louarn, H. de Santana, *J. Mater. Sci.: Mater. Electron.* **27**, 5371 (2016)
30. S. Sakamoto, M. Okumura, Z. Zhao, Y. Furukawa, *Chem. Phys. Lett.* **412**, 395 (2005)